DELPHI Collaboration DELPHI 2001-087 CONF 515
June 25, 2001

Search for Single Top Production at LEP via Four-Fermion Contact Interactions at $\sqrt{s} = 189 - 208$ GeV

Preliminary

S. Andringa[1], N. Castro[1], P. Gonçalves[1], O. Oliveira[2], A. Onofre[1,3], L. Peralta[1], M. Pimenta[1], B. Tomé[1] and F. Veloso[1]

[1]LIP-IST-FCUL, Av. Elias Garcia, 14, 1, P-1000 Lisboa, Portugal
[2]Dep. Física, Universidade de Coimbra, P-3004-516 Coimbra, Portugal
[3]UCP, R. Dr. Mendes Pinheiro, 24, P-3080 Figueira da Foz, Portugal

Abstract

A search for single top production via Four-Fermion Contact Interactions is performed using data taken by the DELPHI detector at LEP-II. The data analysed were accumulated at centre-of-mass energies ranging from 189 to 208 GeV with an integrated luminosity of 539 pb^{-1}. No evidence for signal was found. Preliminary limits at 95% confidence level were obtained on the characteristic energy scale, Λ, for scalar, vector and tensor like couplings.

Contributed Paper for EPS HEP 2001 (Budapest) and LP01 (Rome)

1 Introduction

The study of the top quark properties is one of the main tasks of present high energy physics. In e^+e^- collisions at LEP-II, top quarks can only be singly produced, due to the limited centre-of-mass energy. This production can occur in the Standard Model (SM) via the process $e^+e^- \to e^+\nu_e\bar{t}b\,(e^-\bar{\nu}_e t\bar{b})$. A complete tree level calculation has shown that the corresponding cross-section is $\approx 10^{-6}$ pb, for a top mass around 175 GeV [1].

Single top quarks could also be produced via Flavour Changing Neutral Currents (FCNC). In the SM, FCNC are absent at tree level but, due to Cabbibo-Kobayashi-Maskawa (CKM) mixing, can naturally appear at one-loop level. The smallness of the non-diagonal CKM matrix elements and the relative suppression of the loop contributions make the total FCNC production cross-section very small ($\sigma \approx 10^{-12}$ pb at 200 GeV [2]). In SM extensions like, for instance, supersymmetry [3] and multi-Higgs doublet models [4], the FCNC vertices are present already at tree level. In these models the top quark is expected to play an important role in the understanding of FCNC. A very general procedure is to consider single top quark production in the effective Lagrangian approach via Four-Fermion Contact Interactions [5], as was done by Fermi long time ago.

The most prominent signature for the direct observation of FCNC processes is the single top quark production (together with a charm or up quark) in the reaction $e^+e^- \to t\bar{c}$ (or $e^+e^- \to t\bar{u}$)[1] [6].

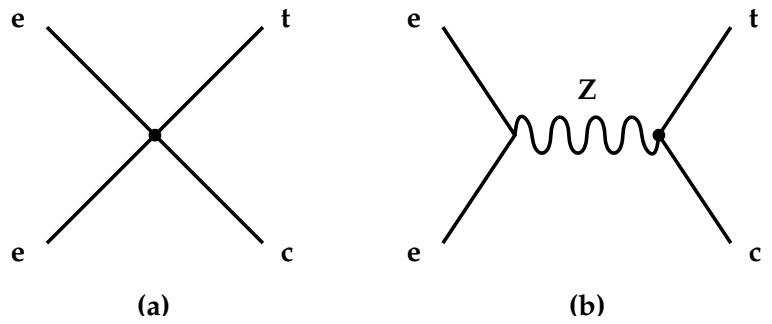

Figure 1: *Feynman diagrams that give rise to $e^+e^- \to t\bar{c}$ in the presence of (a) a new Four-Fermion Contact Interaction Coupling and (b) a new Ztc coupling.*

For the $e^+e^- \to t\bar{c}$ Four-Fermion Contact Interaction (figure 1 a), the differential cross-section can be obtained from the Lagrangian given in [5] and expressed in terms of scalar (S_{RR}), vector (V_{ij} ; $i,j = L,R$) and tensor (T_{RR}) couplings:

$$\begin{aligned}\frac{d\sigma}{d\theta} = \frac{\mathcal{C}}{8}\sin\theta \Big\{ \quad & 2\left(V_{RR}^2 + V_{LL}^2\right)\left[1 + (1+\beta)\cos\theta + \beta\cos^2\theta\right] \\ & + 2\left(V_{RL}^2 + V_{LR}^2\right)\left[1 - (1+\beta)\cos\theta + \beta\cos^2\theta\right] \\ & + S_{RR}^2\,(1+\beta) \\ & - 4S_{RR}T_{RR}\,(1+\beta)\,\cos\theta \\ & + 16T_{RR}^2\left(1 - \beta + 2\beta\cos^2\theta\right) \qquad \Big\} \end{aligned} \tag{1}$$

[1]To make the notation easier, throughout this paper $t\bar{c}$ (and $t\bar{u}$) is to be understood as the final state $t\bar{c} + \bar{t}c$ (and $t\bar{u} + \bar{t}u$).

Couplings	T_{RR}	S_{RR}	V_{RR}	V_{RL}	V_{LR}	V_{LL}	a_R^Z	a_L^Z
scenario 1	1	1	1	1	1	1	0	0
scenario 2	1	0	0	0	0	0	0	0
scenario 3	0	1	0	0	0	0	0	0
scenario 4	0	0	1	1	1	1	0	0
scenario 5	0	0	0	0	0	0	1	1
scenario 6	0	0	1	1	1	1	1	1
scenario 7	0	0	1	1	1	1	-1	-1

Table 1: *Scenarios considered for the scalar, vector and tensor four-fermion couplings*

where

$$\mathcal{C} = \frac{s}{\Lambda^4}\frac{\beta^2}{4\pi(1+\beta)^3} \quad ,$$

$$\beta = \frac{(s-m_t^2)}{(s+m_t^2)}$$

and Λ is the typical energy scale for the process. It should be noted that in the equation (1) only the final state $t\bar{c}$ (not $\bar{t}c$) is considered and the color factor is not included.

The total production cross-section (charge conjugate and color factor included) is obtained by integrating the equation (1):

$$\sigma = \mathcal{C}\ [8T_{RR}^2(3-\beta) + \frac{3}{2}S_{RR}^2(1+\beta) + (V_{LL}^2 + V_{RR}^2 + V_{RL}^2 + V_{LR}^2)(3+\beta)] \qquad (2)$$

If a general $e^+e^- \rightarrow t\bar{c}$ Four-Fermion Contact Interaction exists, it is also possible that a new Ztc vertex (figure 1 b) could exist, being characterized by two new coupling constants, a_L^Z and a_R^Z. The effect of this new vertex could be incorporated in the general Contact Interaction terms by redefining V_{ij} [5]:

$$V_{ij} \rightarrow V_{ij} + 4c_i^Z a_j^Z \frac{m_W m_Z}{s - m_Z^2} \qquad (3)$$

where $i,j = L,R$, $c_L^Z = -1/2 + \sin^2(\theta_W)$ and $c_R^Z = \sin^2(\theta_W)$.

The description of such a Ztc vertex in terms of an anomalous coupling, κ_Z, can be found in [7]. The relation between this coupling and a_L^Z and a_R^Z is given by:

$$\kappa_Z^2 = \left[2\cos(\theta_W)\left(\frac{v}{\Lambda}\right)^2\right]^2 (a_L^{Z^2} + a_R^{Z^2}) \ , \qquad (4)$$

where v is the SM vacuum expectation value. DELPHI also quotes limits in κ_Z versus the anomalous γtc coupling, κ_γ, in [6].

The scenarios studied, considering relevant different types of couplings, are summarized in table 1. The total cross-section at $\Lambda = 1$ TeV is plotted in figure 2 for these scenarios.

At LEP-II the centre-of-mass energies ($\sqrt{s} = 189 - 208$ GeV) are well above the $t\bar{c}$ production threshold, which gives the possibility to perform a direct search for $e^+e^- \rightarrow t\bar{c}$ Four-Fermion Contact Interactions. In this process, the t-quark is expected to decay mainly into Wb. Only the leptonic decays of the W are considered in this note.

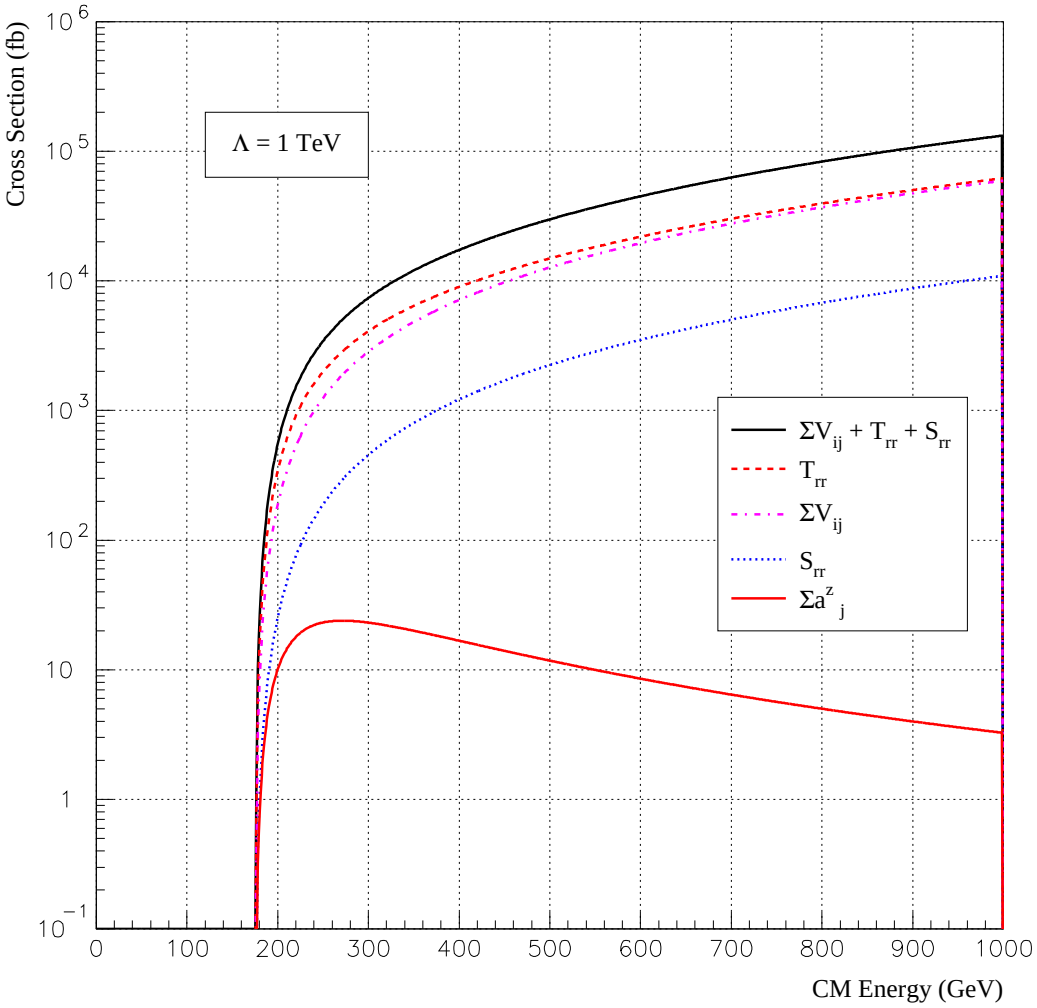

Figure 2: *Total cross-section,* $\sigma_{tc} = \sigma(e^+e^- \to t\bar{c} + \bar{t}c)$ *(in fb) as function of the centre-of-mass energy for* $\Lambda = 1$ *TeV. The following scenarios are considered:* $V_{LL} = V_{LR} = V_{RL} = V_{RR} = S_{RR} = T_{RR} = 1$ *(dark solid line), only* $T_{RR} = 1$ *(long-dashed line), only the four vector couplings* $V_{ij} = 1$ *(dot-dashed line), only* $S_{RR} = 1$ *(dotted line) and only both* $a_j^Z = 1$ *(light solid line). It should be noted that the scenarios* $V_{ij} = a_j^Z = 1$ *(table 1, scenario 6) and* $V_{ij} = 1\,; a_j^Z = -1$ *(table 1, scenario7), if plotted, would be coincident with the four vector couplings* $V_{ij} = 1$.

2 Data Analysis and Event Selection

The data used were collected with the DELPHI detector [8] at $\sqrt{s} = 189 - 208$ GeV and correspond to an integrated luminosity of 539 pb^{-1}. The luminosity collected for each energy is shown in table 2.

The background process $e^+e^- \to Z\gamma$ was generated with PYTHIA 6.125. For $\mu^+\mu^-(\gamma)$ and $\tau^+\tau^-(\gamma)$, DYMU3 [9] and KORALZ 4.2 [10] were used, respectively, while the BHWIDE generator [11] was used for Bhabha events. Simulation of four-fermion final states was performed using EXCALIBUR [12] and grc4f [13]. Two-photon interactions giving hadronic final states were generated using TWOGAM [14]. The generated signal and background events were passed through the detailed simulation of the DELPHI detector and then processed with the same reconstruction and analysis programs as the real data. The numbers of simulated events from different background processes were several times the numbers in the real data.

The final state in the semileptonic channel (with $W \to l\nu$) corresponding to the single top production is characterized by two jets and one well isolated and energetic lepton. In order to improve efficiency, lower momentum isolated leptons were also allowed in the event. The jet coming from the b-quark is expected to be energetic, while the other jet is of low momentum. This signal was generated using a modified version of PYTHIA [15], where the angular distribution for t-quark production was introduced according to equation (1).

In order to identify the semileptonic channel a discriminating analysis, described in detail in [6], was used. At the pre-selection level, the event topology was defined using the number of jets, isolated leptons and photons. The events were accepted if they had at least 7 good tracks and at least one charged lepton with hits on the vertex detector. The most energetic lepton was assumed to come from the leptonic decay of W. Using the Durham algorithm [16], all particles except the charged lepton were forced into two jets. Additionally, the events were required to satisfy the following conditions:

- the visible energy had to be higher than 20% of the centre-of-mass energy;
- the momenta of the most energetic lepton and of the most energetic jet had to be greater than 5 GeV/c;
- the missing energy had to be greater than 30 GeV;
- the polar angles of the lepton and the jets had to be above 10° and below 170°;
- the polar angle of the missing momentum had to be above 10° and below 170°;
- the combined b-tag parameter [17] had to be greater than -2.

Assuming a $jjl\nu$ final state, energy-momentum conservation can be imposed, assigning the missing momentum to the undetected neutrino. After the kinematic fit, the top mass would be given by the invariant mass of the most energetic jet, the lepton and the neutrino.

Events with χ^2 lower than 7 were accepted, provided the mass of the two jets and the mass reconstructed with the missing momentum and the isolated lepton momentum were both below 120 GeV/c^2.

After the pre-selection level, a discriminating variable was constructed using the following variables:

- momentum of the less energetic jet;
- combined event b-tag variable;
- reconstructed mass of the two jets;
- reconstructed top mass;
- angle between the two jets;
- lepton-neutrino invariant mass;
- $q_l \cdot \cos\theta_l$, where q_l is the charge and θ_l is the polar angle of the lepton;
- $q_{j1} \cdot \cos\theta_{j1}$, where $q_{j1} = -q_l$ and θ_{j1} is the polar angle of the most energetic jet;
- $p_{j1} \cdot [\sqrt{s} - p_{j1}(1 - \cos\theta_{j1\,j2})]$, where p_{j1} is the momentum of the most energetic jet and $\theta_{j1\,j2}$ is the angle between the two jets.

Correlations between these variables were studied and no visible effect on the discriminating variable was seen. Table 2 shows, at the pre-selection level and for different centre-of-mass energies, the number of data candidates and the number of expected background events. For all energies and scenarios considered, the efficiencies convoluted with the leptonic branching ratio of the W are between $(16 \pm 1)\%$ and $(17 \pm 1)\%$ (pre-selection level).

$\sqrt{s}$ (GeV)	DATA (SM EXPECTATION)	luminosity (pb $^{-1}$)
189	389 (418 ± 8)	151.8
192	72 (71 ± 1)	25.9
196	216 (216 ± 4)	76.5
200	229 (234 ± 4)	83.5
202	93 (112 ± 2)	40.1
205	194 (217 ± 5)	78.8
207	187 (229 ± 5)	84.3

Table 2: *Number of data candidates and expected background events for different energies at the pre-selection level. The luminosity for each energy is also shown. For* $\sqrt{s} \approx 205$ *GeV and* $\sqrt{s} \approx 207$ *GeV the data was collected during the year 2000 (above* $\sqrt{s} = 202$ *GeV) and splited into 2 energy bins, below and above* $\sqrt{s} = 206$ *GeV, respectively.*

Some distributions for data, background and signal are shown in figures 3 and 4. For each event, a signal likelihood (P_S) and background likelihood (P_B) probability were computed and the discriminating variable was defined as $\log(P_S/P_B)$.

In figure 5 the number of events of data and SM are plotted for all energies as a function of the cut in the discriminating variable.

As an example, likelihood ratio distributions for data, SM and signal are plotted for scenario 1 (figure 6) at $\sqrt{s} \approx 205$ GeV .

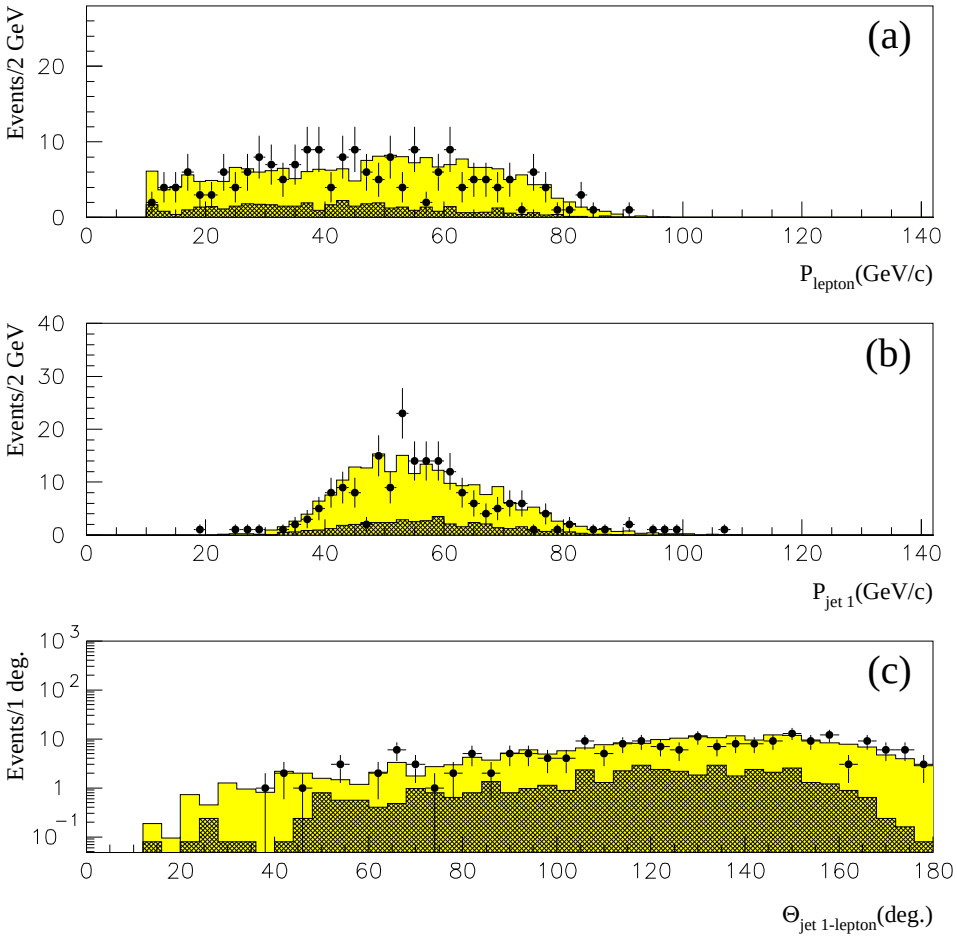

Figure 3: *Distributions (for data, expected background and signal at $\sqrt{s} \approx 205$ GeV) at the pre-selection level of the a) momentum of the lepton, b) momentum of the most energetic jet and c) angle between the most energetic jet and the lepton.*

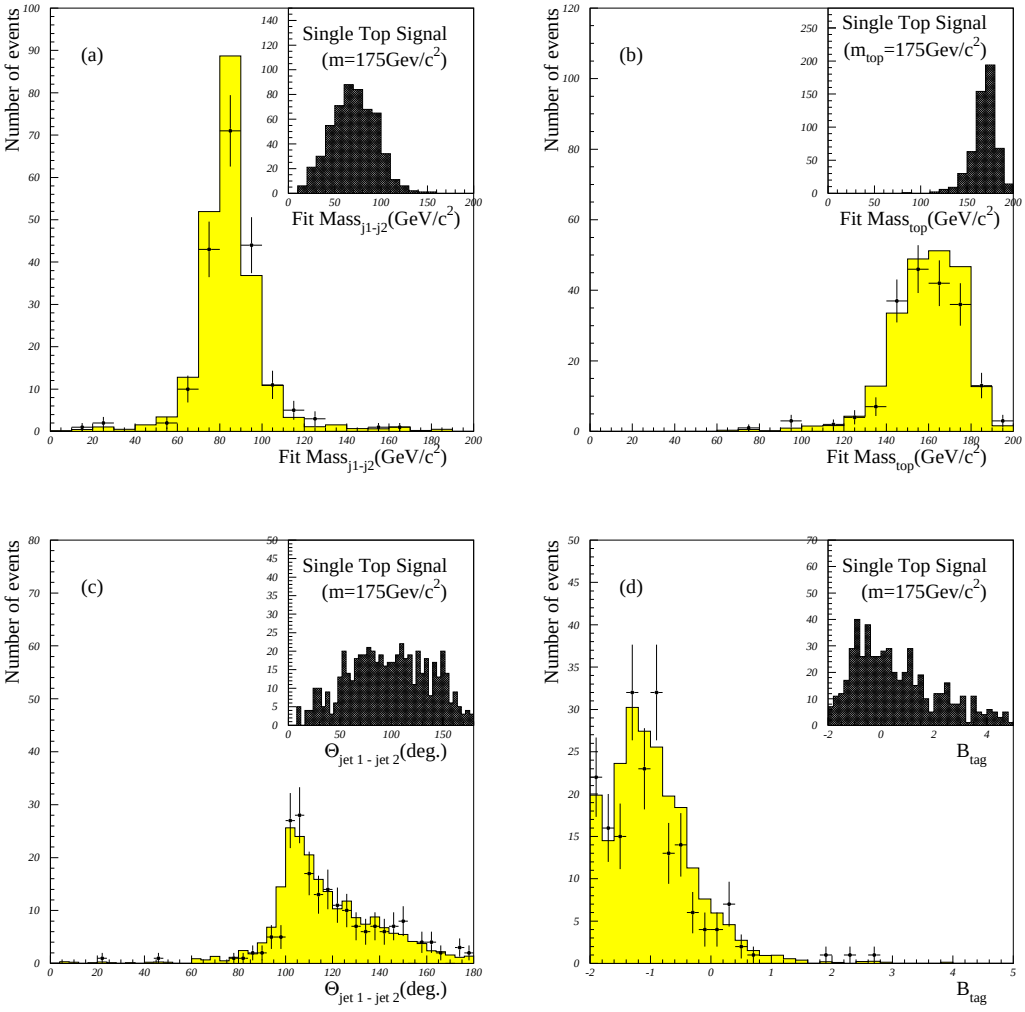

Figure 4: *Distributions (for data, expected background and signal at $\sqrt{s} \approx 205$ GeV) at the pre-selection level of the a) fitted mass of the two jets, b) fitted mass of the top quark, c) angle between the two jets and d) b-tag parameter. The mass resolution for a) and b) is ≈ 9 GeV.*

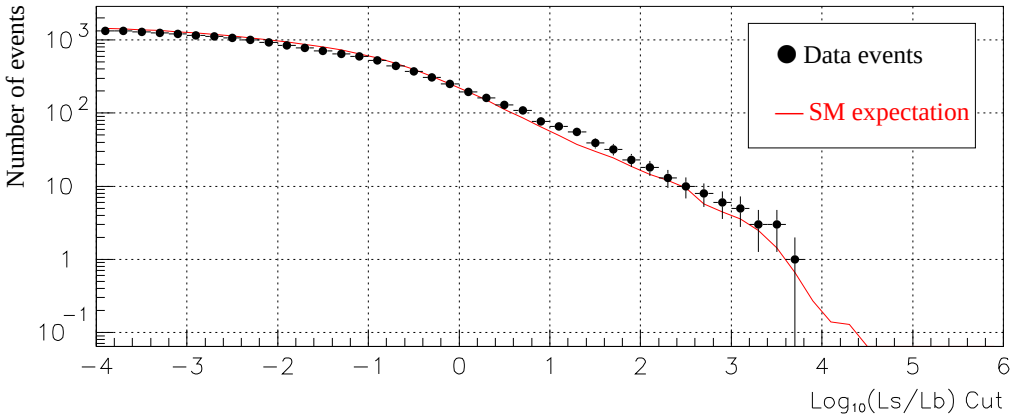

Figure 5: *Number of events of data and expected from SM as function of the cut in the discriminating variable, log(P_S/P_B), for all energies ($\sqrt{s} = 189 - 208$ GeV).*

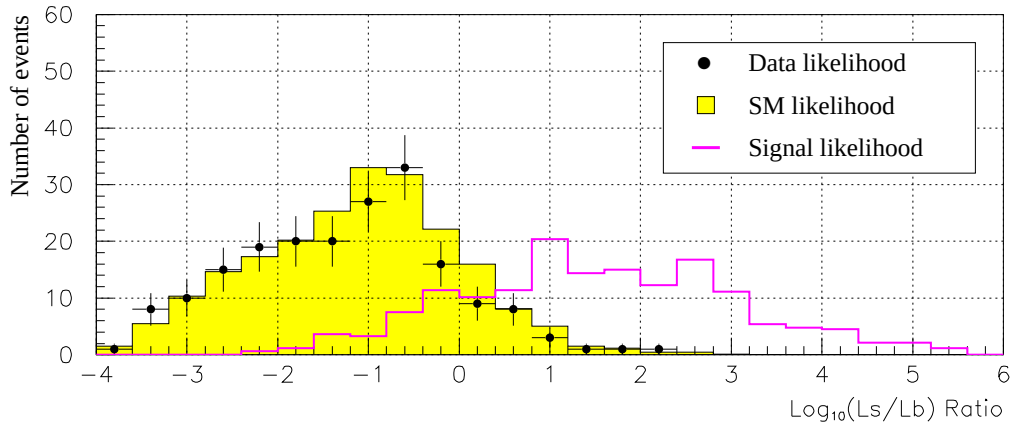

Figure 6: *Data, expected background and signal likelihood ratios for scenario 1 ($T_{RR} = S_{RR} = V_{ij} = 1\,; a_j^Z = 0\,; i,j = L,R$) at $\sqrt{s} \approx 205$ GeV. For the other scenarios, the signal likelihoods do not change significantly.*

3 Results and conclusion

The combination of the data collected with the DELPHI detector at centre-of-mass energies from 189 GeV to 208 GeV shows no evidence for a Four-Fermion Contact Interaction signal. Preliminary limits on the energy scale, Λ, were obtained (at 95% confidence level) by the likelihood ratio method described in [18], for each of the considered scenarios. In addition to the number of candidates and the expected signal and background levels,

the values at the pre-selection level of the discriminating variables for data, signal and background were used. These limits are shown in table 3. The cross-section limit for $\sqrt{s} \approx 207$ GeV is ≈ 0.25 pb for all the considered scenarios. No directly comparable limits in Λ were found in the literature.

scenario $(i, j = L, R)$	observed limit (GeV)	expected limit (GeV)
1) $T_{RR} = S_{RR} = V_{ij} = 1\,;\, a_j^Z = 0$	1312	1423
2) $T_{RR} = 1\,;\, S_{RR} = V_{ij} = a_j^Z = 0$	1143	1253
3) $S_{RR} = 1\,;\, T_{RR} = V_{ij} = a_j^Z = 0$	604	660
4) $T_{RR} = S_{RR} = 0\,;\, V_{ij} = 1\,;\, a_j^Z = 0$	986	1069
5) $T_{RR} = S_{RR} = V_{ij} = 0; a_j^Z = 1$	473	510
6) $T_{RR} = S_{RR} = 0\,;\, V_{ij} = a_j^Z = 1$	992	1083
7) $T_{RR} = S_{RR} = 0\,;\, V_{ij} = 1; a_j^Z = -1$	1003	1092

Table 3: *Observed and expected limits in Λ at 95% confidence level obtained in this analysis.*

References

[1] Boos E. at al, *Phys. Lett.* **B326** (1994) 190.

[2] Huang C.S., Wu X.H. and Zhu S.H., *Phys. Lett.* **B452** (1999) 143.

[3] Divitiis G.M. et al in *IIème Rencontre de Physique de la Vallée d'Aoste: Results and Perspectives in Particle Physics, La Tuille, Italy, 2-8 Mar. 1997*, ed. Greco, M. - INFN, Frascati (1997).

[4] Atwood D., Reina L. and Soni, A., *Phys. Rev.* **D53** (1995), no. 3, pp. 1199-1201.

[5] Bar-Shalom S. and Wudka J., *Phys. Rev.*, **D60** (1999) no. 9, pp.094016/1-14.

[6] DELPHI coll., Andringa S. et al., DELPHI 2001-020 CONF 461 (2001).

[7] Obraztsov V.F., Slabospitsky S.R. and Yushchenko O.P., *Phys. Lett.* **B426** (1998) 393.

[8] DELPHI coll., Aarnio P. et al., *Nucl. Instr. Meth.* **A303** (1991) 233;
DELPHI coll., Abreu P. et al., *Nucl. Instr. Meth.* **A378** (1996) 57.

[9] Campagne J.E. and Zitoun R., *Z. Phys.* **C43** (1989) 469.

[10] Jadach S., Ward B.F.L. and Was Z., *Comp. Phys. Comm.* **79** (1994) 503.

[11] Jadach S., Placzek W. and Ward B.F.L., *Phys. Lett.* **B390** (1997) 298.

[12] Berends F.A., Pittau R., Kleiss R., *Comp. Phys. Comm.* **85** (1995) 437.

[13] Fujimoto J. et al., *Comp. Phys. Comm.* **100** (1997) 128.

[14] Nova S., Olchevski A, and Todorov T., "TWOGAM, a Monte Carlo event generator for two photon physics", DELPHI Note 90-35 PROG 152.

[15] Sjöstrand T., *Comp. Phys. Comm.* **82** (1994) 74.

[16] Catani S. et al., *Phys. Lett.* **B269** (1991) 432.

[17] Borisov G. *Nucl. Instr. Meth.* **A417** (1998) 384.

[18] DELPHI coll., Read, A.L., DELPHI 97-158 PHYS 737 (1997).